Received: September 16, 2019

INASS

International Journal of
Intelligent Engineering & Systems

http://www.inass.org/

A Novel Approach to Detect the Acute Lymphoblastic Leukemia Based on the Color Orthonormal Basis Entropy (COBE) and the Distribution of the Pixel Intensity (DoPI)

Arif Muntasa[1]* **Muhammad Yusuf[1]**

[1]*Informatics Engineering Department,*
University of Trunojoyo Madura, Raya Telang PO BOX 2, Bangkalan, 69162, Indonesia
* Corresponding author's Email: arifmuntasa@trunojoyo.ac.id

Abstract: One of the most dangerous cancer is acute leukemia lymphoblastic (ALL). This type of leukemia has been attacking the most of children. This research aims to detect the ALL diseases through the principal features of the object. Furthermore, this paper contributes by providing a new approach to detect the ALL disease based on the Color Orthonormal Basis Entropy (COBE) and the Distribution of the Pixel Intensity (DoPI). There are some novelties in this research. Firstly, we combined three channels features to characterize an object for increasing the performance accuracy. Secondly, we have developed a model to improve the image through a contrast enhancement filter, the noises from the image can be recognized and removed automatically, and better image result has been delivered through enhancement of the green channel selection. In this research, we proposed a novel approach to detect the ALL based on the COBE and the DoPI. This new approach is divided into four main stages, i.e., image enhancement, segmentation, feature extraction, and performance measurements. Firstly, an image was enhanced through a channel separation, enhancement of the green channel, and fusion of the green channel enhancement with the original channel, i.e., the red and blue channels. An image enhancement process is conducted by a gamma correction of the contrast stretching. The hue channel is an output of the first stage. Secondly, the Otsu algorithm was employed to obtain the best threshold. Thirdly, the COBE and the DoPI were included to discover the main features. Lastly, the Manhattan method was employed to measure performance. In this research, the second Acute Lymphoblastic Leukemia-Image Database (The 2nd ALL-IDB, usually it is called as ALL-IDB2). It is carried out to evaluate the proposed approach. The results show this proposed method has produced high accuracy at 91.67% and small standard deviation at 0.022.

Keywords: Acute leukemia lymphoblastic, Image enhancement, Orthonormal basis entropy, Otsu algorithm.

1. Introduction

One of the most dangerous cancer is Leukemia, especially acute leukemia lymphoblastic (ALL). It is also called as lymphoblasts and cancer of white blood cells (WBC) or bone marrow [1, 2]. This disease can be identified by the overproduction of lymphocytes in the blood. ALL mostly attacks children at 2 to 5 years old [2, 3]. Therefore, early and quick detection of the cancer is urgent for the treatment of the patient. Some symptoms can be diagnosed through medical checks, such as bone pain, anemia, and fever. There are various detection methods, such as manual by pathologist and haematologist, while automatic using image processing methods as computer-aided diagnosis (CAD) [2]. The healthy or infected white blood cells (WBC) can be classified and detected by the CAD system [4]. Therefore, it is important for complementary early and manual detection.

There are existing researches related to the detection methods of leukemia disease, particularly ALL that have been developed by other researchers, i.e. [1] proposed a novel scheme using a Gray level co-occurrence matrix and random forest-based for ALL recognition. It has accuracies at 96.29%, for segmentation, 99.004% for classification and 96 %

for cytoplasm and nucleus in each specific part, [2] applied local binary pattern (LBP) features for lymphocyte cell classification. Image classification was conducted using the SVM classifier to identify the blast or normal cell. The experiment result shows this classification method produced better accuracy. However, [2] has two limitations, which are Linear Binary Pattern (LBP) only captured the small object. Secondly, [2] also has applied the features based on the ratio, i.e., the solidity, compactness, the ratio between cytoplasm and nucleus areas, and the ratio of the nucleus and cell area. All of the features based on the ratio have weaknesses, such as two objects with different sizes and have the same ratio will be assumed as objects with similar features. This concept will produce a false result when the similarity measurement is conducted, even though it used the SVM as the classifier.

[3] utilized a global contrast stretching (GCS) and segmentation based on HSI (Hue, Saturation and Intensity) color space to enhance the color, quality. The result points out the proposed method performed a good segmentation performance on ALL and AML, [5] examined ALL segmentation using the C-Y color space method. The proposed algorithm has segmentation accuracy at 98.38% in comparison with the manual process. It utilizes 100 microscopic ALL images. This method has good segmentation accuracy, [6] conducted a classification of the normal white blood cells from the affected cells in a microscopic image using texture feature. The experiment shows the proposed technique has very good accuracy at 99.66%, [7] proposed approach based on image processing techniques through full leucocyte isolation and divided the nucleus and cytoplasm. Then, the new approach extracted shape, color, and texture. These features were utilized for leukemia detection through different classification models. This proposed method has 92% accuracy for leucocyte recognition. Therefore, it has very good accuracy and efficiency. [8] employed a fuzzy-based two-phase color segmentation scheme. This scheme has been used to separate leukocytes or WBC from other blood segments. It also utilized nucleus shape and texture for the last recognition of leukemia.

Furthermore, Hausdorff Dimension and contour signature are also used for lymphocytic cell nucleus classification. Then, the SVM classifier is applied for Leukemia recognition with the proposed features. The result is 93% accuracy using the SVM classifier, [9] employed the GLCM as feature extraction and the SVM as a binary classifier to conduct image segmentation. The method has utilized 11 vector lengths and delivered 72.4% and 56.1% detection accuracies for a nucleus and cytoplasm. However, if the vector length is changed into13, then the method has produced 72.4 % and 86.7% accuracies for nucleus and cytoplasm. Additionally, the researcher also fused the feature vector as 37, and then it has yielded 89.8% accuracy, [10] employed watershed transform and two simpler classification models to identify the existence of the ALL in blood precisely. The result points out a good accuracy for a normal and blast lymphocytic cell differentiation using this approach. Also, other researches have been conducted, such as [11] captured a quantitative microscopic approach and SVM classifier to detect the ALL and the Acute Myeloid Leukemia (AML). [12] pointed out imaging flow cytometry for diagnosing acute leukemia. [13] captured Two Bare-bones Particle Swarm Optimization (BBPSO) algorithms for ALL diagnosis. [14] employed Fuzzy C-Means based on morphological contour segmentation for Leukemia detection. [15] examined a Gaussian-mixtures blending for clustering cell groups in flow cytometric data. [16] proposed a deep sequencing approach for ALL detection. [17] captured PSO and Adaptive K-nearest neighborhood method for cancer classification small round blue cell tumor (SRBCT) data, the ALL and the AML data and mixed-lineage leukemia (MLL) data. [18] employed a fuzzy mix-prototype (FMP) clustering for microarray of leukemia data analysis. [19] described color image enhancement methods for leukemia classification between the ALL and the AML. [20] applied another method such as ensemble particle swarm model selection (EPSMS) for the morphological classification of acute leukemia. [21] proposed a classification for Acute Leukemia using SVM and K-Means Clustering. [22] employed an ensemble classifier system for ALL detection in advance. [23] employed blood smear images and a neural classifier for the ALL detection. [24] has utilized shape models to obtain the main features, which are area, perimeter, the ratio between square perimeter and area (it is called as compactness), and the ratio between $4\pi \times area$ and square perimeter (it is named as form factor). These features are similar to [2], where two or more objects with multiple perimeters and areas will have same ratio. Then, those objects will be considered as objects with similar features. If the produced features are measured the similarity, then it will generate an incorrect result [24].

Based on the literature review, we defined a problem that there is limited research capture object representation, where it has an impact on the

similarity measurement result. Therefore, this research employed the Color Orthonormal Basis Entropy (COBE) and the Distribution of the Pixel Intensity (DoPI). These methods have not been implemented in the previous literature. Therefore, this work has novelty on our proposed method comparing to the existing technique. In our pre-processing method, the original information has been preserved, so that the lost information can be minimized, whereas the previous research has employed an original image (24 bit) to greyscale image (8 bit). Therefore, much information has been lost as the image conversion process.

Furthermore, this research aims to develop a model for the ALL based on the COBE and DoPI approaches. Hopefully, this paper contributes a novel approach for the ALL detection based on the COBE and the DoPI. Also, this paper implies theory, such as this research adds the novel approaches to the body of knowledge of the ALL, leukemia, computer science, computer vision, biometrics, and image processing fields. Moreover, this research has some novelties as follows: (1) Fusion of three color channels features has increased the accuracy performance. (2) The developed model of contrast enhancement filter can distinguish significantly between main and background objects. (3) The proposed model can detect and remove the noises from the image. Therefore, the resulted feature extractions have better precision. (4) Enhancement of the green channel selection has delivered better image results than all of the channel improvement.

The brief structure of the paper is divided into four sections as follows: introduction, proposed method, result, and discussion, as well as a conclusion. The first section of this paper will examine the background, literature reviews, gaps, aim, contribution, implications, and novelties of the research. The second section will describe the proposed method and the flow chart of each stage. The third section will capture the experimental results, analysis, and discussion of the performance. The fourth section will point out the conclusion, limitations of the proposed method and future research.

2. Proposed method

This section describes the details of our proposed method, which consists of four main stages, i.e., image enhancement as shown in Fig. 1, segmentation as appeared in Fig. 2, feature extraction as described in Fig. 3, and performance measurements. The flowchart of each stage is also shown in this section.

Firstly, image enhancement is carried out to improve the image quality. A color image can be represented using a matrix as follows:

$$F_{r,g,b} = \begin{pmatrix} f(1,1,(r,g,b)) & \cdots & f(1,n,(r,g,b)) \\ \vdots & \ddots & \vdots \\ f(m,1,(r,g,b)) & \cdots & f(m,n,(r,g,b)) \end{pmatrix} \quad (1)$$

$F_{r,g,b}$ represents a color image, where it has three channels, i.e., red (F_r), green (F_g), and blue channels (F_b).

However, the image quality plays an important role to obtain the maximum accuracy. The image enhancement process can be initialized through splitting the channel, i.e., red, green, and blue channels as follows.

$$F_r = \begin{pmatrix} f(1,1,r) & \cdots & f(1,n,r) \\ \vdots & \ddots & \vdots \\ f(m,1,r) & \cdots & f(m,n,r) \end{pmatrix} \quad (2)$$

$$F_g = \begin{pmatrix} f(1,1,g) & \cdots & f(1,n,g) \\ \vdots & \ddots & \vdots \\ f(m,1,g) & \cdots & f(m,n,g) \end{pmatrix} \quad (3)$$

$$F_b = \begin{pmatrix} f(1,1,b) & \cdots & f(1,n,b) \\ \vdots & \ddots & \vdots \\ f(m,1,b) & \cdots & f(m,n,b) \end{pmatrix} \quad (4)$$

The image improvement is only conducted on the green channel after an image channel separation, while the red and blue channels are not necessary to be improved. The green channel improvement (G_g) is employed to add contrast stretching by gamma correction. In this case, we used the value range between 0 and 1 [0,1]. The improvement result $(G_{r,g,b})$ is fused to original red and blue channels as follows:

$$G_{r,g,b} = (F_r, G_g, F_b) \quad (5)$$

Eq. (5) described a combination of three channels, i.e., an original red channel, enhancement result of the green channel, and original blue channel. Many studies have proven that improvement using the green channel is better than three channels, i.e., red, green, and blue channels. Furthermore, the image result is converted to the HSV model. Finally, we selected the hue channel the HSV as the final results on the first stage, as shown in Fig.1. The role of the first stage is important, as a mistake of the pre-processing algorithm will impact the next process. In this case, we employe a green channel only to

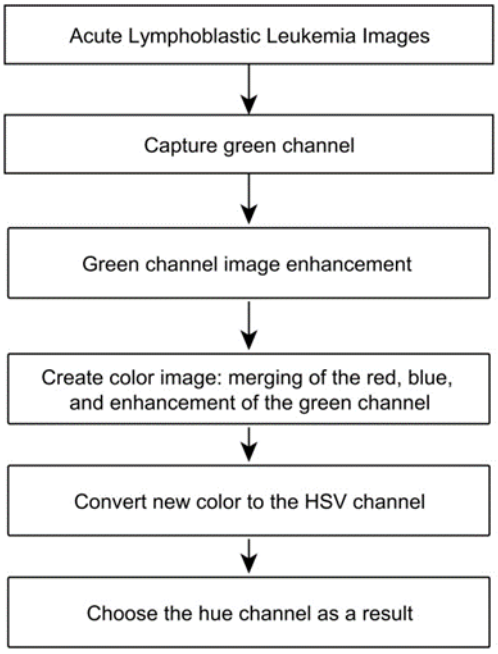

Figure. 1 Image enhancement of our proposed method

improve an original image before the segmentation process, as the green channel can separate the main object and the image background.

Secondly, we conducted an image segmentation, as shown in Fig. 2. A crucial problem of image segmentation is more than two objects have been produced. We have combined the hue channel and an original image as the input to gain the best segmentation result. The hue image channel is improved through a contrast enhancement filter. The process can appear as an edge of the main object. Moreover, we converted into a binary image using the Otsu method. The Otsu method is an algorithm to determine the best threshold value of the image based on the pixel distribution of the object. The Otsu threshold can be expressed using the following equation:

$$\sigma_w^2(t) = \omega_b(t) + \sigma_w^2(t) + \omega_f(t) \times \sigma_f^2(t) \quad (6)$$

$$\sigma_B^2(t) = \omega_b(t) \times \omega_f(t) \times \left(\mu_b(t) - \mu_f(t)\right)^2 \quad (7)$$

The threshold value can be found the maximum of an Eq. (6) or a minimum of Eq. (7). The $\sigma_w^2(t)$ and $\sigma_B^2(t)$ correspond to the *Within* and *between Class Variance*. The weight of foreground and background are stated using $\omega_f(t)$ and $\omega_b(t)$, whereas the mean of the foreground and background are represented using $\mu_f(t)$ and $\mu_b(t)$.

However, the binary image process has delivered many objects. Therefore, we have chosen the biggest object as the main object, i.e., a combination of the nucleus and cytoplasm, as shown in the following algorithm 1. Variable of *NumOfObject* states the number of objects found of the image

Algorithm 1. The biggest object area selection algorithm

```
Area←9999
Counter←0
while Counter< NumOfObject
        Counter←Ciounter+1
        if Object(Counter)>Area
                Area ← Object(Counter)
                Index←Counter
        end if
end while
```

We employed *Object*(*index*) as the biggest (for example, *C* is the biggest object) to be further processed. Our proposed method ensures that the image segmentation results cannot change from the original object, i.e., nucleus and cytoplasm, while unimportant objects have been removed and changed into the background.

The multiplier coefficient can be computed as follows:

$$MC = 255 \times (\sim C) \quad (8)$$

Moreover, we reduced the brightness of the original image using the multiplier coefficient (MC) as follows:

$$H_r = F_r - MC \quad (9)$$

$$H_g = F_g - MC \quad (10)$$

$$H_b = F_b - MC \quad (11)$$

In this case $H_r, H_g,$ and H_b are the brightness result of the red, green, and blue channels. Further, the segmentation result $\left(S_{r,g,b}\right)$ of the second stage can be represented using the following equation:

$$S_{r,g,b} = RGB\left(H_r, H_g, H_b\right) \quad (12)$$

Thirdly, we employed the segmentation result to acquire the object feature. We proposed the various orthonormal basis entropy, i.e., *Energy* (EN), *Entropy* (EP), *Shanon Entropy* $\left(H(X)\right)$, and *Log Energy Entropy* (EE) as follows:

$$EN = \sum_{i=0}^{H-1} \sum_{j=0}^{W-1} \left(S_{r,g,b}(i,j)\right)^2 \quad (13)$$

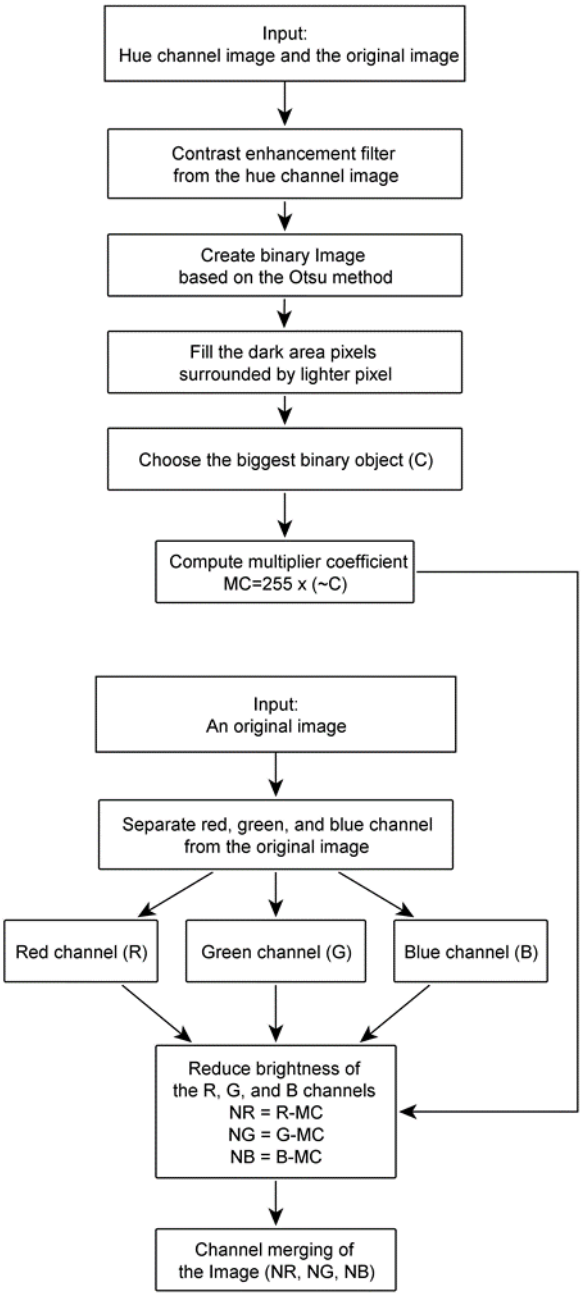

Figure. 2 Image segmentation of our proposed method

$$EP = -\sum_{i=0}^{H-1}\sum_{j}^{W-1} S_{r,g,b}(i,j) \times log\left(S_{r,g,b}(i,j)\right) \quad (14)$$

$$H(X) = -\sum_{i=1}^{n} P(x_i) log_b\, P(x_i) \quad (15)$$

$$EE = -\sum_{i=1}^{n} P_i log(P_i) \quad (16)$$

In Eqs. (13) and (14), the variable of W and H states the width and height of an image, while $S_{r,g,b}$ represents an image segmentation result.

Table 1. Confusion matrix

Actual Value	Classifier Prediction	
	Positive	**Negative**
Positive	True Positive	False Negative
Negative	False Positive	True Negative

Random values are stated using X. In Eq. (15) and (16), we found the value of X. It has a range $\{x_1, x_2, \cdots, x_n\}$, while symbol of log_b and $P(x_i)$ state logarithm base and probability mass function. Additionally, we also employed the distribution of the pixel intensity to characterize the object, i.e., variance (VA) *and* Correlation (CO) as follows:

$$VA = \sum_{i=0}^{H-1}\sum_{j}^{W-1}(i-\mu) \times S_{r,g,b}(i,j) \quad (17)$$

$$CO = \sum_{i=0}^{H-1}\sum_{j}^{W-1}\frac{(i-\mu_x)\times(j-\mu_y)}{\sigma_x \times \sigma_y} \quad (18)$$

The variable of μ and σ state mean and standard deviation.

In this research, we employed the color image segmentation results to extract the main feature each channel, i.e., the red, green, and blue channels. $\mathcal{F}$ and $\mathcal{H}$ represent the features of the training and testing sets. The use of those channels is to maximize the characterized features.

The use of those channels is to maximize the characterized features.

Lastly, we detected acute leukemia lymphoblastic based on the various orthonormal basis entropy and the distribution of the pixel intensity. We applied the Manhattan method to measure the similarity of the features as follows:

$$D_{Manhattan} = |\mathcal{F} - \mathcal{H}| \quad (19)$$

We utilized the confusion matrix to calculate accuracy. This method is employed to evaluate the reliability and consistency of the proposed method.

$$Accuracy = \frac{TP+TN}{TP+TN+FP+FN} \quad (20)$$

TP states true positive, where classifier prediction and actual value are positive. If classifier prediction and actual value are negative, then it is called as true negative (*TN)*. If classifier prediction is positive and actual value is stated as negative, then it is called as false positive (*FP*). Otherwise, it is called false negative (*FN*), as shown in Table 1.

3. Results and discussions

This section will point out the experimental result of red, green, and blue channels using Manhattan methods. It also captures some figures for the performance of the experiments and analysis.

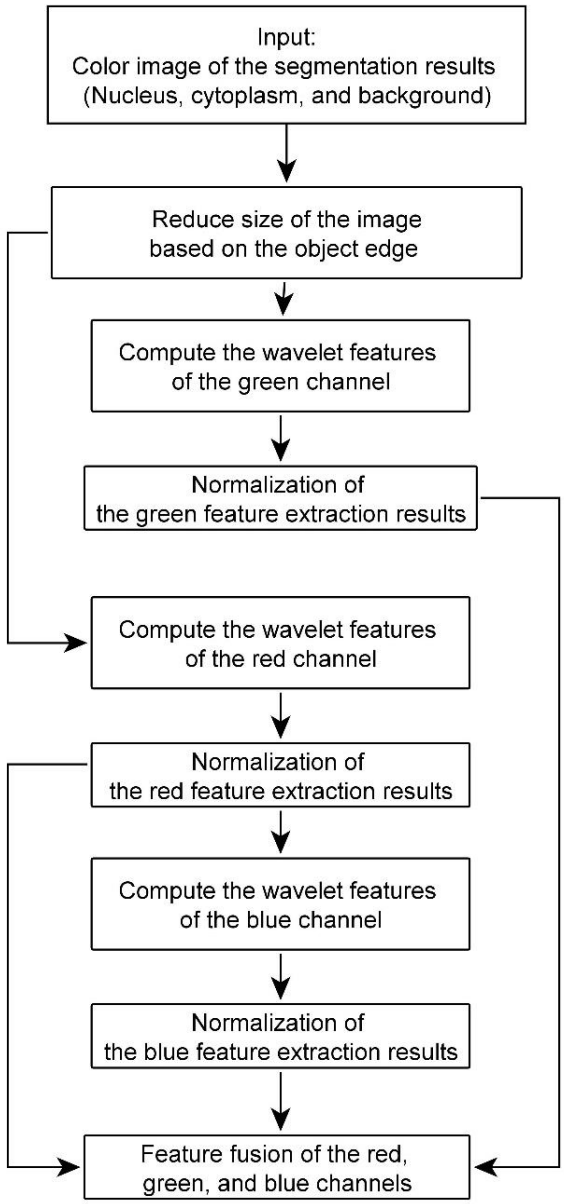

Figure. 3. Extraction model of our proposed method

We employed an Acute Lymphoblastic Leukemia-Image Database (ALL-IDB) to evaluate the proposed method. The All-IDB has captured 260 images, where 130 images are positive of the ALL, whereas the rest of the images are negative. Table 2 depicts the scenario of our experiments.

In Table 2, the characters of R, G, and B represent the red, green, and blue channels. Also, the word of RGB depicts the true color channel.

In this research, we detected separately the ALL using red, green, and blue channels. Also, we combined all features of the red, green, and blue channels as shown in the last column of Table 2. The first column shows several of used training sets. Each class is multiplied to two (negative and positive the ALL). Similarly, it can be seen in the second column. The third, fourth, and fifth columns describe an evaluation using the features of the red, green, and blue channels. The last column states the evaluation using feature fusion of the red, green and blue channels. We have randomly selected the index of the training sets as ten times. The ALL image samples can be seen in Fig. 4. Four images on the first row infected positive of the ALL, while the second row consists of the negative of the ALL.

Image enhancement results will determine the quality of the image segmentation. Our proposed method was able to improve the main object and remove unimportant other objects so that the main object can be easily separated into the background.

Our proposed method can separate clearly between the main object and background during segmentation. Better segmentation results will give effect to the next processes, which are feature extraction and similarity measurement.

We employ the information theory to obtain the main features of the object, which are *Energy*, *Entropy*, *Shanon Entropy*, and *Log Energy Entropy*. Also, we involved *Variance* and *Correlation* to distinguish the pixel distribution, whether leukemia or not.

3.1. Experimental results of the red channel using manhattan

We have conducted the experiments to evaluate and detect the ALL using red channel features,

Table 2. Scenarios of the proposed method evaluation

Number of the training sets	**Number of the testing sets**	**Cross-Validation Experiment**			
		R	**G**	**B**	**RGB**
56 × 2 = 112	74 × 2 = 148	10	10	10	10
57 × 2 = 114	73 × 2 = 146	10	10	10	10
58 × 2 = 116	72 × 2 = 144	10	10	10	10
59 × 2 = 118	71 × 2 = 142	10	10	10	10
60 × 2 = 129	70 × 2 = 140	10	10	10	10
61 × 2 = 122	69 × 2 = 138	10	10	10	10
62 × 2 = 124	68 × 2 = 136	10	10	10	10
63 × 2 = 126	67 × 2 = 134	10	10	10	10
64 × 2 = 128	66 × 2 = 132	10	10	10	10
65 × 2 = 130	65 × 2 = 130	10	10	10	10

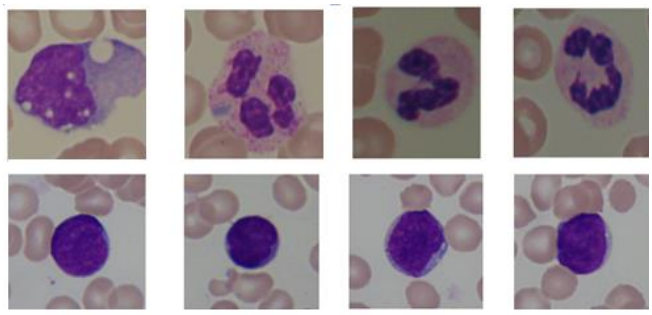

Figure. 4 The ALL-IDB Samples. The above images are Positive ALL, while the bottom images are Negative ALL [1]

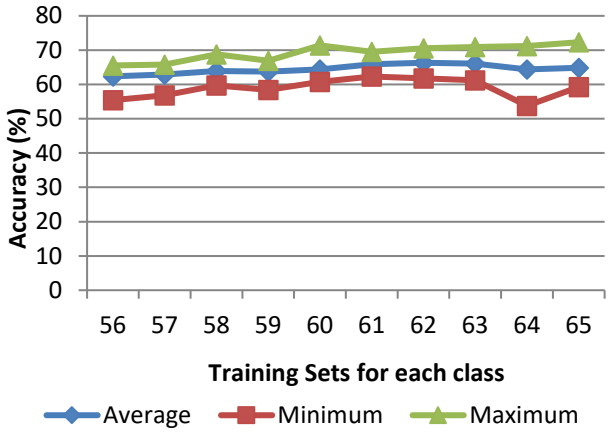

Figure. 5 Performance of the red channel to detect the ALL

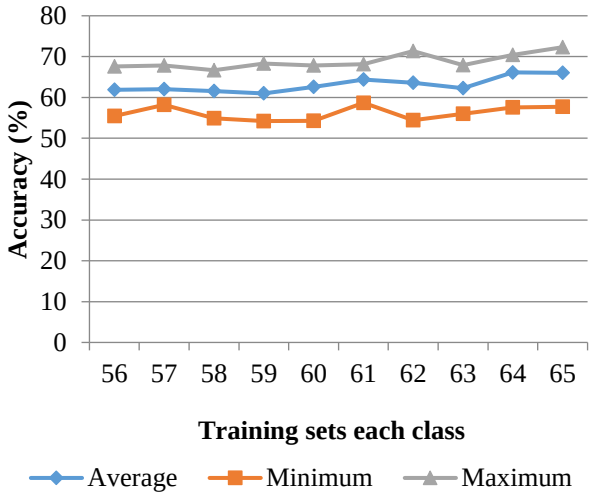

Figure. 6 Performance of the green channel to detect the ALL

where a number of the used features are six. We have conducted ten experiments for different training sets as displayed in Table 2. The experimental results have been concluded, i.e., the minimum, average, and maximum accuracies, as shown in Fig. 5. It shows that the best accuracies of the average, minimum, and maximum, are 66.32%, 62.32%, and 72.31%, respectively, whereas the produced standard deviation is 0.024. In general, several training sets have influenced the obtained accuracy. The more training sets are applied, the higher accuracy is obtained, even though there are two anomaly points, i.e., 59 and 61 features of the maximum accuracy. Then, the minimum accuracy also decreases, when 64 features are applied.

The experiment was conducted using a different index of the training sets. Each experiment could produce different accuracy, even though it has employed the same number of training sets. However, the difference between the produced accuracy for each experiment is not significant. It can be shown by the produced standard deviation value, i.e., 0.024

3.2. Experimental results of the green channel using Manhattan

Similarly, we also employed to extract the green channel features using orthonormal basis entropy and the distribution of the pixel intensity. The results show the best average, minimum, and maximum accuracies are 66.14%, 58.69%, 72.31%, as shown in Fig. 6. The results of the green channel have delivered a similar accuracy with the red channel. It can be concluded the red and green channels have similar features. The difference between the training set index has produced different accuracy. Therefore, the delivered results are also different. It can be shown from the different standard deviation for each channel. In this case, the green channel has delivered 0.031 of the standard deviation.

3.3. Experimental results of the blue channel using manhattan

The best average, minimum, maximum, and standard deviation are 72, 65.38, 78.46, and 0.02. The last separation feature extraction is the blue channel. It has delivered better accuracy than the red and blue channels. The results show that the average, minimum, and maximum accuracies are 72%, 65.38%, and 78.46% as described in Fig. 7. The increasing of the accuracy has been clearly shown, where the best average accuracy increased from 66.14% to 72%. The best average also increases from 58.69% to 65.38% accuracy, while the best maximum accuracy increases from 72.31% to 78.46%. It shows that the blue channel has delivered much information than red or green channels. Therefore, the blue channel has increased by 7% the accuracy.

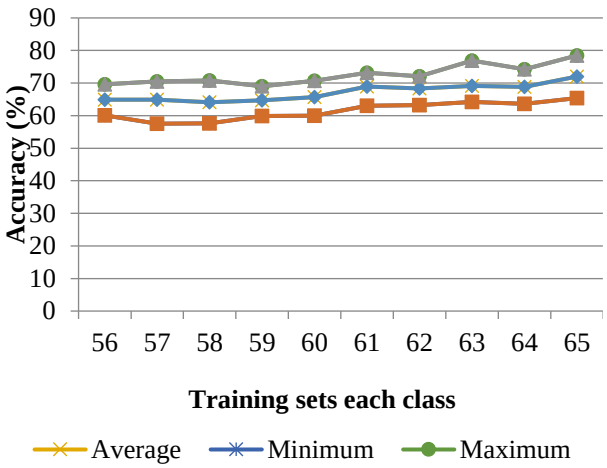

Figure. 7 Performance of the blue channel to detect the ALL

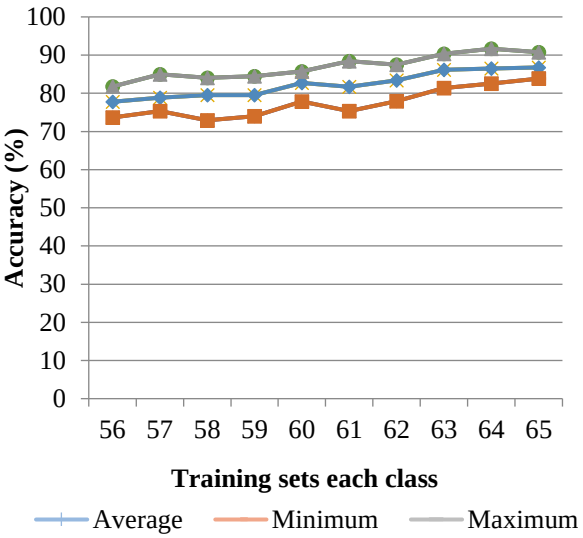

Figure. 8 Performance of the color channel to detect the ALL

3.4. Experimental Results of the color image using Manhattan

The last experiment is a combination of red, green, and blue channel features. We fused all features, where each channel has six features. When we blend three channels, the number of the utilized features is eighteen features. The results show that the best average, minimum, and maximum and standard deviation are 86.77%, 83.85%, and 91.67%, respectively. Our proposed method has delivered the results, as shown in Fig. 8.

The results have produced better accuracy than the red, green, or channel, i.e. the best average, minimum, and maximum accuracies, as shown in Fig. 9. It shows that the best maximum accuracy has

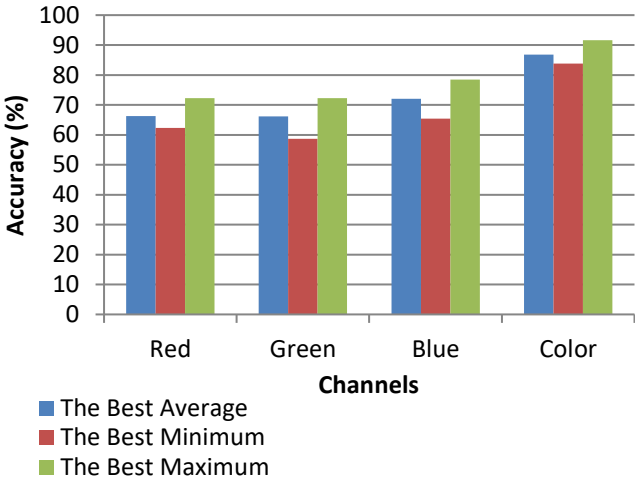

Figure. 9. Performance of the best of the red, green, blue, and color channels to detect the ALL

increased more than 19% after the red, green, and blue channel features are fused. Also, the utilized of the color channel features has increased by more than 20% and 25% for the best average and minimum accuracies. The proposed method has delivered 0.022 standard deviations of the maximum accuracy on the color experiments. It shows that the proposed method has produced stable maximum accuracy.

The increasing of the detection accuracy on the color channel features is influenced by appearance important object information after the red, green, and blue channels are mixed. The unity of the red, green, and blue features can patch the loss information for each channel. However, the separation of the color channel features caused loss information of the object. The effect of the loss information has caused the object cannot powerfully characterized, therefore the object is correctly unrecognized.

3.5. The comparison results in other researches

In this research, we applied all of the ALL-IDB2 as the data experiments to evaluate our algorithm. We conducted some experiments as shown in Table 2. Also, we selected randomly the training sets ten times. It is conducted to evaluate the reliability of our proposed method. Furthermore, the experiments are carried out for each channel (red, green, and blue channels) and combining the channels. However, [24] only employed 20 images for positive of the ALL, and 20 images for negative of the ALL, whereas [2] utilized 75 images for positive of the ALL and 65 images for negative of the ALL for the training sets. Additionally, the rest of the images have been applied as the testing sets.

We have compared our results to other previous researches [2] [24]. [2] has detected the ALL using some instruments as follows:

a) Area
b) Perimeter
c) Convex area
d) Eccentricity
e) Major axis length
f) Minor axis length
g) Orientation
h) Solidity, the ratio between area and convex area see Eq. (1) in [2])
i) Compactness, the ratio between square parameter and convex area see Eq. (1) in [2])
j) The ratio between cytoplasm and nucleus areas
k) The ratio of the nucleus and cell area

The last four instruments are h), i), j), and k). These instruments have limitations, which are it produced a similar ratio from two images that have different objects. Also, [2] assumed that those two images and objects with the same ratios are considered as the same objects. However, the actual conditions are different. Therefore, the produced result delivered a false decision, even though many researchers have employed the support vector machine to classify the object. However, the produced accuracy is less than our proposed method result. The result shows the accuracy of 88.79% for the shape features.

The local Binary Pattern (LBP) method [2] also has some limitations. The LBP only captures a small object area. Also, the LBP cannot handle all of the main object areas, so that many information have losses and fail to represent the main object. From a mathematics perspective, even though it uses Naive Bayesian and Support Vector Machine methods to measure the similarity of the main object, then it is getting difficult to recognize the object as the more important features are lost [24].

[2, 24] did not capture execution time and calculation volume, therefore we did not compare those parameters. There is no comparison about computation time as the processing machine getting faster nowadays, so that it is not an issue.

Our features employed the whole of the statistical model so that our proposed method can capture the main object correctly. We do not employ the shape model to extract the features as utilized in [2].

There are a lot of similarities in shape between the infected and uninfected ALL. Furthermore, the use of the LBP also has limitations, i.e., the infected and uninfected ALL have similarities texture.

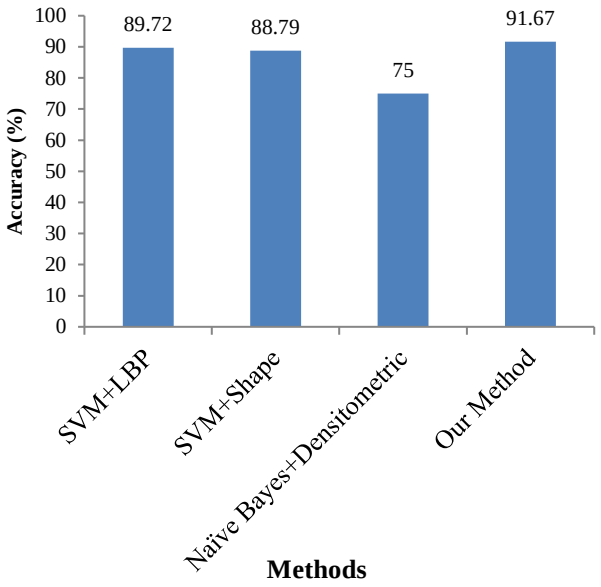

Figure. 10 Comparison result between our proposed method and the others

Moreover, [3] also has utilized the area, perimeter, compactness, and form factor as the shape features and energy, entropy, correlation, and variance as densitometric features. Additionally, the infected and uninfected ALL have higher similarities in shape. Therefore, the Naïve Bayes method can be distinguished between the infected and uninfected ALL. The method delivered 75 % accuracy as it combined. Furthermore, a complete comparison can be seen in Fig. 10.

Fig. 10 describes our proposed method has outperformed to other methods, which are SVM-LBP, SVM-Shape, and Naïve Bayes-Shape + Densitometric. The novel method has proven that the fusion of three channels can represent the whole object of the image.

4. Conclusion

This section will examine the summary and conclusion of the research, limitations of the proposed method and future research. Based on the experimental result, our proposed method has produced maximum accuracy at 91.67%. Also, our proposed method has delivered 0.022 standard deviations for the color image. It means the difference of our accuracy results between scenarios is small.

The experimental results depicted that the proposed method has produced better accuracy than the channel separation, i.e., the red, green, and blue channels. The increase of the accuracy in the average, minimum, and maximum are more than 20%, 25%, and 19%, respectively. The increasing of

the accuracy indicated that the fusion of the red, green, and blue channels had delivered important information to identify the acute lymphoblastic leukemia.

The proposed method has limitations, i.e., firstly, the use of the object features without a selection process. Secondly, features of the object only reflect a texture appearance of the object, while the shape of the object is not considered as important information. Lastly, the similarity measurement only considers the distance between pixels of the image. We will involve the shape as the principal features in future research. Besides, we will select the most important feature, embed the weight of the features, and remove unimportant information as well. Furthermore, we will employ the neural network and its development as a similarity measurement.

Acknowledgments

We would like to thank the Directorate of Higher Education – Ministry of research, technology and higher education for supporting our research under the Basic Research Funding Scheme 2018. This paper is a part of our research project. Also, thank you very much goes to Computational Artificial Intelligence and Business Intelligent System Laboratories at Informatics Engineering Department, Engineering Faculty, University of Trunojoyo Madura, Indonesia.

References

[1] S. Mishra, B. Majhi, P. K. Sa, and L. Sharma, "Gray level co-occurrence matrix and random forest based acute lymphoblastic leukemia detection", *Biomed. Signal Process. Control*, Vol. 33, pp. 272–280, Mar. 2017.

[2] V. Singhal and P. Singh, "Local Binary Pattern for automatic detection of Acute Lymphoblastic Leukemia", In: *Proc. of 2014 20th Natl. Conf. Commun. NCC 2014*, 2014.

[3] N. H. A. Halim, M. Y. Mashor, A. S. Abdul Nasir, N. R. Mokhtar, and H. Rosline, "Nucleus segmentation technique for acute leukemia", In: *Proc. of 2011 IEEE 7th Int. Colloq. Signal Process. Its Appl. CSPA 2011*, pp. 192–197, 2011.

[4] S. Mishra, B. Majhi, and P. K. Sa, "Texture feature based classification on microscopic blood smear for acute lymphoblastic leukemia detection", *Biomed. Signal Process. Control*, Vol. 47, pp. 303–311, Jan. 2019.

[5] R. Mohammed, O. Nomir, and I. Khalifa, "Segmentation of Acute Lymphoblastic Leukemia Using CY Color Space", *Int. J. Adv. Comput. Sci. Appl.*, Vol. 5, No. 11, pp. 99–101, 2014.

[6] S. Mishra, B. Majhi, and P. K. Sa, "Texture feature based classification on microscopic blood smear for acute lymphoblastic leukemia detection", *Biomed. Signal Process. Control*, Vol. 47, pp. 303–311, 2019.

[7] L. Putzu, G. Caocci, and C. Di Ruberto, "Leucocyte classification for leukaemia detection using image processing techniques", *Artif. Intell. Med.*, Vol. 62, No. 3, pp. 179–191, 2014.

[8] S. Mohapatra, S. S. Samanta, D. Patra, and S. Satpathi, "Fuzzy based blood image segmentation for automated leukemia detection", In: *Proc. of 2011 International Conference on Devices and Communications, ICDeCom 2011 - Proceedings*, 2011.

[9] J. Rawat, A. Singh, H. S. Bhadauria, and J. Virmani, "Computer Aided Diagnostic System for Detection of Leukemia Using Microscopic Images", *Procedia Computer Science*, Vol. 70, pp. 748–756, 2015.

[10] R. Bhattacharjee and L. M. Saini, "Detection of Acute Lymphoblastic Leukemia using watershed transformation technique", In: *Proc. of 2015 Int. Conf. Signal Process. Comput. Control. ISPCC 2015*, No. L, pp. 383–386, 2016.

[11] J. Rawat, A. Singh, B. HS, J. Virmani, and J. S. Devgun, "Computer assisted classification framework for prediction of acute lymphoblastic and acute myeloblastic leukemia", *Biocybern. Biomed. Eng.*, Vol. 37, No. 4, pp. 637–654, Jan. 2017.

[12] L. F. Grimwade, K. A. Fuller, and W. N. Erber, "Applications of imaging flow cytometry in the diagnostic assessment of acute leukemia", *Methods*, vol. 112, pp. 39–45, 2017.

[13] W. Srisukkham, L. Zhang, S. C. Neoh, S. Todryk, and C. P. Lim, "Intelligent leukemia diagnosis with bare-bones PSO based feature optimization", *Appl. Soft Comput.*, vol. 56, pp. 405–419, 2017.

[14] P. Viswanathan, "Fuzzy C Means Detection of Leukemia Based on Morphological Contour Segmentation", *Procedia Computer Science*, 2015, Vol. 58, pp. 84–90.

[15] M. Reiter, P. Rota, F. Kleber, M. Diem, S. Groeneveld-Krentz, and M. Dworzak, "Clustering of cell populations in flow cytometry data using a combination of Gaussian mixtures", *Pattern Recognit.*, Vol. 60, pp. 1029–1040, 2016.

[16] M. Faham, j. Zheng, M. Moorhead, V. Carlton, P. Stow, E. Coustan-Smith, C. Pui, and D. Campana, "Deep-sequencing approach for minimal residual disease detection in acute lymphoblastic leukemia", *Blood*, Vol. 120, No. 26, pp. 5173–5180, 2012.

[17] S. Kar, K. Das Sharma, and M. Maitra, "Gene selection from microarray gene expression data for classification of cancer subgroups employing PSO and adaptive K-nearest neighborhood technique", *Expert Syst. Appl.*, Vol. 42, No. 1, pp. 612–627, 2015.

[18] J. Liu, T. D. Pham, H. Yan, and Z. Liang, "Fuzzy mixed-prototype clustering algorithm for microarray data analysis", *Neurocomputing*, Vol. 276, pp. 42–54, Feb. 2018.

[19] A. N. Aimi Salihah, M. Y. Mashor, N. H. Harun, and H. Rosline, "Colour image enhancement techniques for acute leukemia blood cell morphological features", In: *Proc. of IEEE Int. Conf. Syst. Man Cybern.*, pp. 3677–3682, 2010.

[20] H. Escalante, M. Montes-y-Gómez, J. A. González, P. Gómez-Gil, L. Altamirano, C. A. Reyes, C. Reta, and A. Rosales "Acute leukemia classification by ensemble particle swarm model selection", *Artif. Intell. Med.*, Vol. 55, No. 3, pp. 163–175, 2012.

[21] J. Laosai and K. Chamnongthai, "Acute leukemia classification by using SVM and K-Means clustering", In: *Proc. of 2014 Int. Electr. Eng. Congr. iEECON 2014*, pp. 1–4, 2014.

[22] S. Mohapatra, D. Patra, and S. Satpathy, "An ensemble classifier system for early diagnosis of acute lymphoblastic leukemia in blood microscopic images", *Neural Comput. Appl.*, Vol. 24, No. 7–8, pp. 1887–1904, 2014.

[23] A. Khashman and H. H. Abbas, "Acute Lymphoblastic Leukemia Identification Using Blood Smear Images and a Neural Classifier", International Work-Conference on Artificial Neural Networks, pp. 80-87, 2013.

[24] S. Selvaraj, "Naïve Bayesian classifier for Acute Lymphocytic Leukemia detection Naive Bayesian Classifier for Acute Lymphocytic Leukemia Detection", *ARPN J. Eng. Appl. Sci.*, Vol. 10, No. December, pp. 6888–6892, 2015.